

Estimation of the thickness and the optical parameters of several superimposed thin films using optimization

R. Andrade ^{*} E. G. Birgin [†] I. Chambouleyron [‡] J. M. Martínez [§]
S. D. Ventura [¶]

February 7, 2008

Abstract

The Reverse Engineering problem addressed in the present research consists in estimating the thicknesses and the optical parameters of two thin films deposited on a transparent substrate using only transmittance data through the whole stack. To the present author's knowledge this is the first report on the retrieval of the optical constants and the thickness of multiple film structures using transmittance data only. The same methodology may be used if the available data correspond to normal reflectance. The software used in this work is freely available through the PUMA Project web page (<http://www.ime.usp.br/~egbirgin/puma/>).

Keywords: Optical constants, thin films, optimization, numerical algorithms, Reverse Engineering.

1 Introduction

The problem of estimating the thickness and the optical constants of thin films using transmittance (or reflectance) data only is very challenging from the mathematical point of view and has a technological and an economic importance. It always represents a very ill-conditioned inverse problem with many local-nonglobal solutions. The ill-condition of this reverse engineering process stems from the fact that the available transmittance data for retrieving the structure is incomplete and frequently noisy. So, as in highly underdetermined problems, infinitely unstable or physically meaningless solutions are expected [1]. In

^{*}Department of Computer Science IME-USP, University of São Paulo, Rua do Matão 1010, Cidade Universitária, 05508-090, São Paulo SP, Brazil. e-mail: randrade@ime.usp.br

[†]Department of Computer Science IME-USP, University of São Paulo, Rua do Matão 1010, Cidade Universitária, 05508-090, São Paulo SP, Brazil. e-mail: egbirgin@ime.usp.br

[‡]Department of Applied Physics, Institute of Physics, University of Campinas, CP 6065, 13083-970 Campinas SP, Brazil. e-mail: ivanch@ifi.unicamp.br

[§]Department of Applied Mathematics, IMECC-UNICAMP, University of Campinas, CP 6065, 13081-970 Campinas SP, Brazil. e-mail: martinez@ime.unicamp.br

[¶]Department of Mathematics, ICE-UFRRJ, Federal Rural University of Rio de Janeiro, Km 7, Rodovia BR 465, 23890-000, Seropédica RJ, Brazil. email: damxtha@gmail.com

previous publications we successfully (see [2] for a critical review) addressed the problem of retrieving the optical constants and the thickness of a single dielectric or semiconductor film deposited onto a thick transparent substrate. The inverse problem was solved for thin [3, 4] and for very thin films [5] using spectral transmittance data only. The solution was found introducing an unconstrained formulation of the nonlinear programming model and solving the estimation problem with a method based on repeated calls to an unconstrained minimization algorithm [3]. An extension of the solution of the inverse problem using only reflectance data was recently reported [6].

In the present contribution we address the problem of retrieving the properties of an optical structure that includes more than one dielectric film, deposited either on one side or onto both sides of a transparent substrate of known optical properties. By the properties of the structure we mean the optical constants (extinction coefficient and refractive index, as a function of wavelength) and the thickness of each of the films composing the structure. As in our previous contributions the challenge consists of retrieving the properties of the system using transmittance data only. Note that the degree of underdetermination of the problem increases as the number of films increases.

The paper is organized as follows. In the next section, a general discussion of the mathematical model of the estimation problem is presented. The optimization technique for a couple of thin films is described in Section 3. Section 4 presents numerical experiments and the results obtained with a structure containing two amorphous semiconductor films deposited onto a crystalline silicon substrate. The conclusions are summarized in Section 5.

2 Mathematical model of the estimation problem

The optical structure we have in mind is a stack of thin films deposited on both sides of a transparent substrate. As usually, we define the *top* of the stack as the side where light impinges, the *bottom* being the opposite side. The numerical experiments are performed on transmittance (T) data of computer generated a-si:H and a-Ge:H films calculated using the optical constants given in the Appendix. The transmittance data of *gedanken* films, rounded-off to four digits, were calculated in a $[\lambda_{\min}, \lambda_{\max}]$ nm wavelength interval. The T data of real film structures were measured in a VIS-IR spectrophotometer.

The refractive index s of the transparent substrate is known. The thickness of the substrate is also known but it plays no role in the calculations, the reason being that its thickness is much larger than the wavelengths into play [7, 1]. For each film of the structure the unknowns are the refractive index and the extinction coefficient (in the λ_{\min} to λ_{\max} interval) and its thickness [8, 9].

Assume that $m_t \geq 0$ films are deposited on the top of the substrate and $m_b \geq 0$ films are deposited on the bottom. For all $i = 1, \dots, m_t$, $\lambda \in [\lambda_{\min}, \lambda_{\max}]$, we denote:

$$\begin{aligned} d_i^t &= \text{thickness of top film } i, \\ n_i^t(\lambda) &= \text{refractive index of top film } i, \\ \kappa_i^t(\lambda) &= \text{attenuation coefficient of top film } i. \end{aligned}$$

Analogously, for all $i = 1, \dots, m_b$, $\lambda \in [\lambda_{\min}, \lambda_{\max}]$, we denote:

$$\begin{aligned} d_i^b &= \text{thickness of bottom film } i, \\ n_i^b(\lambda) &= \text{refractive index of bottom film } i, \\ \kappa_i^b(\lambda) &= \text{attenuation coefficient of bottom film } i. \end{aligned}$$

For each wavelength λ , the theoretical transmittance is a function of thicknesses, refractive indices and attenuation coefficients, so:

$$T^{\text{theoretical}}(\lambda) = T(s(\lambda), \{d_i^t\}_{i=1}^{m_t}, \{n_i^t(\lambda)\}_{i=1}^{m_t}, \{\kappa_i^t(\lambda)\}_{i=1}^{m_t}, \{d_i^b\}_{i=1}^{m_b}, \{n_i^b(\lambda)\}_{i=1}^{m_b}, \{\kappa_i^b(\lambda)\}_{i=1}^{m_b}). \quad (1)$$

In order to simplify the notation, we write:

$$\begin{aligned} d_{\text{top}} &= \{d_i^t\}_{i=1}^{m_t}, & n_{\text{top}}(\lambda) &= \{n_i^t(\lambda)\}_{i=1}^{m_t}, & \kappa_{\text{top}}(\lambda) &= \{\kappa_i^t(\lambda)\}_{i=1}^{m_t}, \\ d_{\text{bottom}} &= \{d_i^b\}_{i=1}^{m_b}, & n_{\text{bottom}}(\lambda) &= \{n_i^b(\lambda)\}_{i=1}^{m_b}, & \kappa_{\text{bottom}}(\lambda) &= \{\kappa_i^b(\lambda)\}_{i=1}^{m_b}. \end{aligned}$$

and

$$d_{\text{all}} = \{d_{\text{top}}, d_{\text{bottom}}\}, \quad n_{\text{all}} = \{n_{\text{top}}, n_{\text{bottom}}\}, \quad \kappa_{\text{all}} = \{\kappa_{\text{top}}, \kappa_{\text{bottom}}\}.$$

So, (1) can be written as:

$$T^{\text{theoretical}}(\lambda) = T(s(\lambda), d_{\text{all}}, n_{\text{all}}(\lambda), \kappa_{\text{all}}(\lambda)).$$

When $m_t = 1$ and $m_b = 0$, the formula (1) is the one given in [10] and used in [3, 7, 4] for retrieving the optimal parameters of a single film deposited on the top of a transparent substrate [11]. A general formula for arbitrary m_t and m_b is discussed in Sections 1.4–1.6 of [1]. Proofs that the integrals along thickness of the substrate correspond to the analytical expression shown in [1] can be found in [12]. In this work we use a formula introduced by Ventura [13] which, although equivalent to the ones given in [1] is better suited for numerical computations. In particular, derivatives of the parameters involved in (1) are easily available when we use these formulae. The transmittance of a couple of different films deposited onto a transparent substrate can be expressed in a compact form.

If the two films are deposited onto the same face of the substrate the transmittance reads:

$$T_{FFS} = \frac{64s(n_1^2 + \kappa_1^2)(n_2^2 + \kappa_2^2)x_1x_2}{x_1x_2(Ax_1x_2 + Bx_1 + Cx_2 + D + E) + x_1(Fx_1 + G) + x_2(Hx_2 + I) + J},$$

where

$$\begin{aligned}
A &= -[(n_1 - 1)^2 + \kappa_1^2][(n_2 + n_1)^2 + (\kappa_2 + \kappa_1)^2][(s^2 - n_2)(n_2 - 1) - \kappa_2^2], \\
B &= 2[(n_1 - 1)^2 + \kappa_1^2][B_s \sin(\varphi_2) - B_c \cos(\varphi_2)], \\
B_s &= \kappa_2(s^2 + 1)(n_2^2 - n_1^2 + \kappa_2^2 - \kappa_1^2) - 2(n_2^2 + \kappa_2^2 - s^2)(\kappa_2 n_1 - \kappa_1 n_2), \\
B_c &= (\kappa_2^2 + n_2^2 - s^2)(n_2^2 - n_1^2 + \kappa_2^2 - \kappa_1^2) + 2\kappa_2(s^2 + 1)(\kappa_2 n_1 - \kappa_1 n_2), \\
C &= 2[(s^2 - n_2)(n_2 - 1) - \kappa_2^2][2C_s \sin(\varphi_1) - C_c \cos(\varphi_1)], \\
C_s &= \kappa_1[(n_1^2 + \kappa_1^2 + n_2)(n_2 - 1) + \kappa_2^2] - \kappa_2 n_1(n_1^2 + \kappa_1^2 - 1), \\
C_c &= (n_1^2 + \kappa_1^2 - 1)(n_2^2 - n_1^2 + \kappa_2^2 - \kappa_1^2) + 4\kappa_1(\kappa_2 n_1 - \kappa_1 n_2), \\
D &= 2[(n_2 + n_1)^2 + (\kappa_2 + \kappa_1)^2][D_s \sin(\varphi_1 + \varphi_2) + D_c \cos(\varphi_1 + \varphi_2)], \\
D_s &= 2\kappa_1(n_2^2 + \kappa_2^2 - s^2) + \kappa_2(s^2 + 1)(n_1^2 + \kappa_1^2 - 1), \\
D_c &= 2\kappa_1\kappa_2(s^2 + 1) - (n_2^2 + \kappa_2^2 - s^2)(n_1^2 + \kappa_1^2 - 1), \\
E &= 2[(n_2 - n_1)^2 + (\kappa_2 - \kappa_1)^2][E_s \sin(\varphi_2 - \varphi_1) - E_c \cos(\varphi_2 - \varphi_1)], \\
E_s &= \kappa_2(s^2 + 1)(n_1^2 + \kappa_1^2 - 1) - 2\kappa_1(n_2^2 + \kappa_2^2 - s^2), \\
E_c &= 2\kappa_1\kappa_2(s^2 + 1) + (n_2^2 + \kappa_2^2 - s^2)(n_1^2 + \kappa_1^2 - 1), \\
F &= [(n_1 - 1)^2 + \kappa_1^2][(n_2 - n_1)^2 + (\kappa_2 - \kappa_1)^2][(s^2 + n_2)(n_2 + 1) + \kappa_2^2], \\
G &= -2[(s^2 + n_2)(n_2 + 1) + \kappa_2^2][2G_s \sin(\varphi_1) - G_c \cos(\varphi_1)], \\
G_s &= \kappa_1(n_2^2 - n_1^2 + \kappa_2^2 - \kappa_1^2) + (\kappa_2 n_1 - \kappa_1 n_2)(n_1^2 + \kappa_1^2 - 1), \\
G_c &= -4\kappa_1(\kappa_2 n_1 - \kappa_1 n_2) + (n_2^2 - n_1^2 + \kappa_2^2 - \kappa_1^2)(n_1^2 + \kappa_1^2 - 1), \\
H &= -[(n_1 + 1)^2 + \kappa_1^2][(n_2 - n_1)^2 + (\kappa_2 - \kappa_1)^2][(s^2 - n_2)(n_2 - 1) - \kappa_2^2], \\
I &= 2[(n_1 + 1)^2 + \kappa_1^2][I_s \sin(\varphi_2) + I_c \cos(\varphi_2)], \\
I_s &= 2(n_2^2 + \kappa_2^2 - s^2)(\kappa_2 n_1 - \kappa_1 n_2) + (s^2 + 1)\kappa_2(n_2^2 - n_1^2 + \kappa_2^2 - \kappa_1^2), \\
I_c &= 2\kappa_2(s^2 + 1)(\kappa_2 n_1 - \kappa_1 n_2) - (n_2^2 + \kappa_2^2 - s^2)(n_2^2 - n_1^2 + \kappa_2^2 - \kappa_1^2), \\
J &= [(n_1 + 1)^2 + \kappa_1^2][(n_2 + n_1)^2 + (\kappa_2 + \kappa_1)^2][(s^2 + n_2)(n_2 + 1) + \kappa_2^2],
\end{aligned}$$

and

$$\beta_1 = \frac{4\pi d_1}{\lambda}, \quad \beta_2 = \frac{4\pi d_2}{\lambda}, \quad \varphi_1 = \beta_1 n_1, \quad \varphi_2 = \beta_2 n_2, \quad x_1 = \exp(-\beta_1 \kappa_1), \quad x_2 = \exp(-\beta_2 \kappa_2).$$

If the two-films are deposited onto different sides of the transparent substrate, the compact formula for the transmittance is:

$$T_{FSF} = \frac{64s(n_1^2 + \kappa_1^2)(n_2^2 + \kappa_2^2)x_1 x_2}{x_1 x_2 (Ax_1 x_2 + Bx_1 + Cx_2 + D + E) + x_1 (Fx_1 + G) + x_2 (Hx_2 + I) + J},$$

where

$$\begin{aligned}
A &= -[(n_1 - 1)^2 + \kappa_1^2][(n_2 - 1)^2 + \kappa_2^2][n_2(n_1^2 + \kappa_1^2 + s^2) + n_1(n_2^2 + \kappa_2^2 + s^2)], \\
B &= 2[(n_1 - 1)^2 + \kappa_1^2][B_s \sin(\varphi_2) + B_c \cos(\varphi_2)], \\
B_s &= \kappa_2[2n_1(s^2 - n_2^2 - \kappa_2^2) + (n_1^2 + \kappa_1^2 + s^2)(n_2^2 + \kappa_2^2 - 1)], \\
B_c &= n_1(n_2^2 + \kappa_2^2 - 1)(n_2^2 + \kappa_2^2 - s^2) + 2\kappa_2^2(n_1^2 + \kappa_1^2 + s^2), \\
C &= 2[(n_2 - 1)^2 + \kappa_2^2][C_s \sin(\varphi_1) + C_c \cos(\varphi_1)], \\
C_s &= \kappa_1[(n_2^2 + \kappa_2^2 + s^2)(n_1^2 + \kappa_1^2 - 1) - 2n_2(n_1^2 + \kappa_1^2 - s^2)], \\
C_c &= 2\kappa_1^2(n_2^2 + \kappa_2^2 + s^2) + n_2(n_1^2 + \kappa_1^2 - s^2)(n_1^2 + \kappa_1^2 - 1), \\
D &= 2[\kappa_2(n_1^2 + \kappa_1^2 - s^2) + \kappa_1(n_2^2 + \kappa_2^2 - s^2)][D_s \sin(\varphi_1 + \varphi_2) - 2D_c \cos(\varphi_2 + \varphi_1)], \\
D_s &= 4\kappa_1\kappa_2 - (n_1^2 + \kappa_1^2 - 1)(n_2^2 + \kappa_2^2 - 1), \\
D_c &= \kappa_2(n_1^2 - 1) + \kappa_1(n_2^2 - 1) + \kappa_1\kappa_2(\kappa_1 + \kappa_2), \\
E &= 2[\kappa_1(n_2^2 + \kappa_2^2 - s^2) - \kappa_2(n_1^2 + \kappa_1^2 - s^2)][E_s \sin(\varphi_2 - \varphi_1) - 2E_c \cos(\varphi_2 - \varphi_1)], \\
E_s &= 4\kappa_1\kappa_2 + (n_2^2 + \kappa_2^2 - 1)(n_1^2 + \kappa_1^2 - 1), \\
E_c &= \kappa_1(n_2^2 - 1) - \kappa_2(n_1^2 - 1) + \kappa_1\kappa_2(\kappa_2 - \kappa_1), \\
F &= [(n_1 - 1)^2 + \kappa_1^2][(n_2 + 1)^2 + \kappa_2^2][n_2(n_1^2 + \kappa_1^2 + s^2) - n_1(n_2^2 + \kappa_2^2 + s^2)], \\
G &= -2[(n_2 + 1)^2 + \kappa_2^2][G_s \sin(\varphi_1) + G_c \cos(\varphi_1)], \\
G_s &= -\kappa_1[2n_2(n_1^2 + \kappa_1^2 - s^2) + (n_2^2 + \kappa_2^2 + s^2)(n_1^2 + \kappa_1^2 - 1)], \\
G_c &= n_2(n_1^2 + \kappa_1^2 - s^2)(n_1^2 + \kappa_1^2 - 1) - 2\kappa_1^2(n_2^2 + \kappa_2^2 + s^2), \\
H &= -[(n_1 + 1)^2 + \kappa_1^2][(n_2 - 1)^2 + \kappa_2^2][n_2(n_1^2 + \kappa_1^2 + s^2) - n_1(n_2^2 + \kappa_2^2 + s^2)], \\
I &= -2[(n_1 + 1)^2 + \kappa_1^2][I_s \sin(\varphi_2) + I_c \cos(\varphi_2)], \\
I_s &= -\kappa_2[2n_1(n_2^2 + \kappa_2^2 - s^2) + (n_1^2 + \kappa_1^2 + s^2)(n_2^2 + \kappa_2^2 - 1)], \\
I_c &= n_1(n_2^2 + \kappa_2^2 - s^2)(n_2^2 + \kappa_2^2 - 1) - 2\kappa_2^2(n_1^2 + \kappa_1^2 + s^2), \\
J &= [(n_1 + 1)^2 + \kappa_1^2][(n_2 + 1)^2 + \kappa_2^2][n_2(n_1^2 + \kappa_1^2 + s^2) + n_1(n_2^2 + \kappa_2^2 + s^2)],
\end{aligned}$$

and

$$\beta_1 = \frac{4\pi d_1}{\lambda}, \quad \beta_2 = \frac{4\pi d_2}{\lambda}, \quad \varphi_1 = \beta_1 n_1, \quad \varphi_2 = \beta_2 n_2, \quad x_1 = \exp(-\beta_1 \kappa_1), \quad x_2 = \exp(-\beta_2 \kappa_2).$$

Both formulations lead to Swanepoel's formulation [10] when the thickness of one of the films goes to zero.

The transmittance data are $T^{\text{theoretical}}(\lambda_i)$ or $T^{\text{meas}}(\lambda_i)$ for wavelengths $\lambda_i, i = 1, \dots, N$, where

$$\lambda_{\min} \leq \lambda_1 < \dots < \lambda_N \leq \lambda_{\max}.$$

Ideally, for all $i = 1, \dots, N$, the true parameters should satisfy the equations

$$T^{\text{meas}}(\lambda_i) = T^{\text{theoretical}}(s(\lambda_i), d_{\text{all}}, n_{\text{all}}(\lambda_i), \kappa_{\text{all}}(\lambda_i)). \quad (2)$$

However, this is a system with $(m_t + m_b)(2N + 1)$ unknowns and only N equations; i.e., highly underdetermined. The many degrees of freedom that are inherent to this problem lead us to introduce empirical and phenomenological constraints that must be satisfied

by the properties of the films under consideration. See [3] and [6] for the application of this philosophy to the one-film estimation problem with transmittance and reflectance data, respectively. Namely, instead of considering the nonlinear system (2) we define the optimization problem

$$\begin{aligned} \text{Minimize} \quad & \sum_{i=1}^N [T^{\text{theoretical}}(s(\lambda_i), d_{\text{all}}, n_{\text{all}}(\lambda_i), \kappa_{\text{all}}(\lambda_i)) - T^{\text{meas}}(\lambda_i)]^2 \\ \text{subject to} \quad & \text{Physical Constraints.} \end{aligned} \quad (3)$$

In the one-film case this strategy has been successfully used many times under the PUMA project (see [3, 4, 6] and <http://www.ime.usp.br/~egbirgin/puma/>).

In the present case we use the same constraints that were employed in the one-film case [3], which are suitable for hydrogenated amorphous semiconductor thin films in the neighborhood of their fundamental absorption edge. For completeness, these constraints are described below. We assume that $n(\lambda)$ is the refractive index and $\kappa(\lambda)$ is the attenuation coefficient of a generic film in the stack.

PC1: $n(\lambda) \geq 1$ and $\kappa(\lambda) \geq 0$ for all $\lambda \in [\lambda_{\min}, \lambda_{\max}]$;

PC2: $n(\lambda)$ and $\kappa(\lambda)$ are decreasing functions of λ ;

PC3: $n(\lambda)$ is convex;

PC4: there exists $\lambda_{\text{infl}} \in [\lambda_{\min}, \lambda_{\max}]$ such that $\kappa(\lambda)$ is convex if $\lambda \geq \lambda_{\text{infl}}$ and concave if $\lambda < \lambda_{\text{infl}}$.

In [3] it has been showed that PC1–PC4 will be satisfied if, and only if,

$$\begin{aligned} n(\lambda_{\max}) &\geq 1, & \kappa(\lambda_{\max}) &\geq 0, \\ n'(\lambda_{\max}) &\leq 0, & \kappa'(\lambda_{\max}) &\leq 0, \\ n''(\lambda) &\geq 0 \text{ for all } \lambda \in [\lambda_{\min}, \lambda_{\max}], \\ \kappa''(\lambda) &\geq 0 \text{ for all } \lambda \in [\lambda_{\text{infl}}, \lambda_{\max}], \\ \kappa''(\lambda) &\leq 0 \text{ for all } \lambda \in [\lambda_{\min}, \lambda_{\text{infl}}], \text{ and} \\ \kappa'(\lambda_{\min}) &\leq 0. \end{aligned}$$

As in [3], we eliminate the constraints of the problem by means of a suitable change of variables. So, we write

$$n(\lambda_{\max}) = 1 + u^2, \quad \kappa(\lambda_{\max}) = v^2, \quad (4)$$

$$n'(\lambda_{\max}) = -u_1^2, \quad \kappa'(\lambda_{\max}) = -v_1^2, \quad (5)$$

$$n''(\lambda) = w(\lambda)^2 \text{ for all } \lambda \in [\lambda_{\min}, \lambda_{\max}], \quad (6)$$

$$\kappa''(\lambda) = z(\lambda)^2 \text{ for all } \lambda \in [\lambda_{\text{infl}}, \lambda_{\max}], \text{ and} \quad (7)$$

$$\kappa''(\lambda) = -z(\lambda)^2 \text{ for all } \lambda \in [\lambda_{\min}, \lambda_{\text{infl}}]. \quad (8)$$

To consider the real-life situation, in which data are given by a set of N equally spaced points on the interval $[\lambda_{\min}, \lambda_{\max}]$, we define:

$$h = (\lambda_{\max} - \lambda_{\min}) / (N - 1) \text{ and } \lambda_i = \lambda_{\min} + (i - 1)h \text{ for } i = 1, \dots, N.$$

We will use the notation n_i , κ_i , w_i , and z_i for the estimates of $n(\lambda_i)$, $\kappa(\lambda_i)$, $w(\lambda_i)$, and $z(\lambda_i)$, for all $i = 1, \dots, N$. The discretization of (4–8) gives:

$$n_N = 1 + u^2, \quad v_N = v^2, \quad (9)$$

$$n_{N-1} = n_N + u_1^2 h, \quad \kappa_{N-1} = \kappa_N + v_1^2 h, \quad (10)$$

$$n_i = w_i^2 h^2 + 2n_{i+1} - n_{i+2} \text{ for } i = 1, \dots, N - 2, \quad (11)$$

$$\kappa_i = z_i^2 h^2 + 2\kappa_{i+1} - \kappa_{i+2}, \text{ if } \lambda_{i+1} \geq \lambda_{\text{inff}}, \text{ and} \quad (12)$$

$$\kappa_i = -z_i^2 h^2 + 2\kappa_{i+1} - \kappa_{i+2}, \text{ if } \lambda_{i+1} < \lambda_{\text{inff}}. \quad (13)$$

Let us stress that these constraints must be satisfied by the refractive indices and the attenuation coefficients of all the films.

3 Optimization technique

Problem (3) with the constraints defined by (9–13) is an optimization problem with $(m_t + m_b)(2N + 1)$ variables.

The constraints are represented by the non negativity of the thicknesses and the fact that the inflection points λ_{inff} must be in the range $[\lambda_{\min}, \lambda_{\max}]$. The remaining variables are unconstrained and dimensionless. These are the main reasons to deal with them in a different way than we do with thicknesses and inflection points. Our strategy is to define, for each set of inflection points and each set of thicknesses a different continuous unconstrained optimization problem whose variables are the ones defined by the refractive indices and the attenuation coefficients. As in [3], the unconstrained problems will be solved using the spectral gradient method [14] (see [15] for a comparative study with the spectral conjugate gradient method). The high-level procedure is defined in the following algorithm.

Algorithm 3.1

Step 1. Define a coarse grid with respect to the variables *thicknesses* and *inflection points*.

Step 2. For each point of the grid solve the problem (3),(9–13) where the variables *thicknesses* and *inflection points* are fixed. Obtain the set of thicknesses and the inflection points of the grid that, after solving the unconstrained optimization problems, give the smallest sum of squares.

Step 3. Define a new refined grid in a vicinity of the best thicknesses and best inflection points obtained at Step 2.

Step 4. Solve the unconstrained optimization problems defined by each point of the new grid. Adopt the solution that gives the smallest value of the sum of squares as the output of the algorithm.

For a system with two films, the initial coarse grid for the thickness is given by uniformly distributed points in the box $[d_{\min}^1, d_{\max}^1] \times [d_{\min}^2, d_{\max}^2]$, where d_{\min}^i and d_{\max}^i are (for film i) the lower and upper bound estimates of the film thicknesses, respectively. To estimate the inflection point we proceed in an analogous way: the initial coarse grid is given by uniformly distributed points in the box $[F_{\min}^1, F_{\max}^1] \times [F_{\min}^2, F_{\max}^2]$, where F_{\min}^i and F_{\max}^i are (for film i) the lower and upper bound estimates of the film inflection points, respectively.

It is worth mentioning that according to the PUMA strategy [3, 4, 6] (successfully used in retrieving the optical constants [16, 17, 18, 19]), the minimization problem (3) must be solved for each given trial set $(d_{\text{trial}}^1, d_{\text{trial}}^2, F_{\text{trial}}^1, F_{\text{trial}}^2)$. Moreover, for each trial set of thicknesses and inflection points, the optimization method needs initial estimates for $n(\lambda)$ and $\kappa(\lambda)$. In fact, the method solves the optimization problem starting from several different initial estimations for $n(\lambda)$ and $\kappa(\lambda)$. The generation of each initial estimation is based on the approximation of $n(\lambda)$ and $\kappa(\lambda)$ by a piecewise linear function as in [3].

This amounts a lot of computer work, which increases exponentially with the number of films. For instance, for the case of a 100nm film together with a 600nm film, the trial thicknesses intervals would be [10, 200]nm and [300, 900]nm, respectively (both of them with step 10nm in the coarse grid). This means a total of 1220 grid points. Moreover, for the retrieval made in the spectrum interval [1000, 2000]nm, there would be 11 trial inflection points per film (obtained with step size equal to 100nm). This implies solving problem (3), (9–13) 147, 620 times. If we consider that this is done for each pair of initial estimates of $n(\lambda)$ and $\kappa(\lambda)$ (see [3]), we conclude that at the first run, the problem (3) is solved 885,720 times.

For this reason, we implemented a parallel version of the optimization procedure described above. Parallelization is straightforward, since the optimization problems can be solved independently.

4 Results

All the experiments were run in a grid composed by four 2.4GHz Intel(R) Core 2 Quad and 4GB of RAM memory. We used the language C and the Message Passing Interface (MPI) with the gcc compiler (GNU project C/C++ compiler, version 4.2.1) and the LAM MPI implementation (version 7.1.2). The program was compiled with the optimization compiler option -O3.

4.1 Computer generated films

We performed numerical experiments with two films. Moreover, as in [3], we assume that, for each film, $\lambda_{\text{infl}} = \lambda_{\min}$ is known. We considered the case of films having equal properties as well as films of different nature. The transmittance data originate from the

computer-generated A , B , C and D films introduced in [3], their optical constants being described in the Appendix. In particular:

Film A: Simulates an a-Si:H thin film with $d^{\text{true}} = 100\text{nm}$.

Film B: Identical to Film A except that $d^{\text{true}} = 600\text{nm}$.

Film C: Simulates an a-Ge:H thin film with $d^{\text{true}} = 100\text{nm}$.

Film D: Identical to Film C with $d^{\text{true}} = 600\text{nm}$.

Moreover, g will denote a glass substrate. For example, AgB system will be an optical structure with Film A on top, a thick glass substrate in the middle and Film B on the bottom.

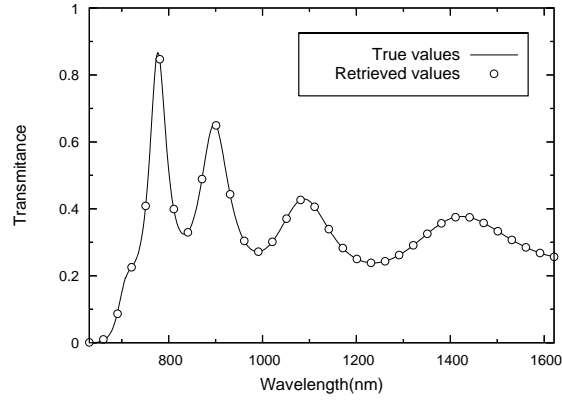
4.1.1 Structures with identical *gedanken* films having the same thickness

The retrieval algorithm was applied to transmittance data of computer generated films simulating the same material and the same thickness. We have two cases; i.e., the structure AAg (or BBg) and the structure AgA (or BgB). Obviously, when both films are deposited onto the same face, top or bottom of the substrate, the algorithm, which supposes two films, is unable to retrieve the true thickness of each of the component films but always retrieve their sum. In other words, for films of identical nature deposited one on top of the other the algorithm find numerous pairs of thicknesses d^1 and d^2 such that $d^1 + d^2 \approx d^{\text{total}}$ that generates the calculated transmittance. Curiously, the same result is obtained when the two films having the same nature and identical thickness are deposited one on top and the other on the bottom of the substrate. The minimization process retrieves films thicknesses the sum of which equals the sum of the individual thickness of the films composing the structure. In other words, there is no trivial way to determine “the pair of thicknesses of the grid that gives the smallest sum of squares”. The optical constants retrieved in this identical-nature identical-thickness films do not correspond, in general, to those used to generate the transmittance. Depending on the thicknesses retrieved n and κ adjust themselves to give an accurate transmittance in the wavelength interval considered. Evidently, if the “true” thickness of one of the films is given, the algorithm finds the “true” thickness of the other one. The correct answer is also found if the algorithm is informed that both films have identical thickness.

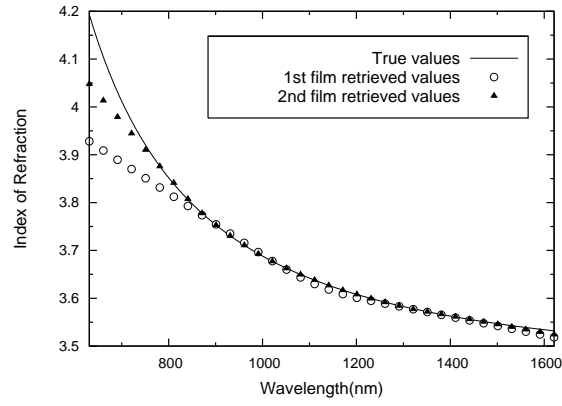
4.1.2 Structures with: a) identical *gedanken* films having different thickness, and b) two films of different nature

In this set of tests, we considered several two-films systems combining a-Si:H and a-Ge:H layers of different thicknesses and deposited on both sides of the glass substrate. The systems considered are: AgB , BgD , CgB and CgD . The spectral ranges used for the retrieval process were: 631–1621nm, 934–1924nm, 817–1807nm and 945–1935nm, respectively.

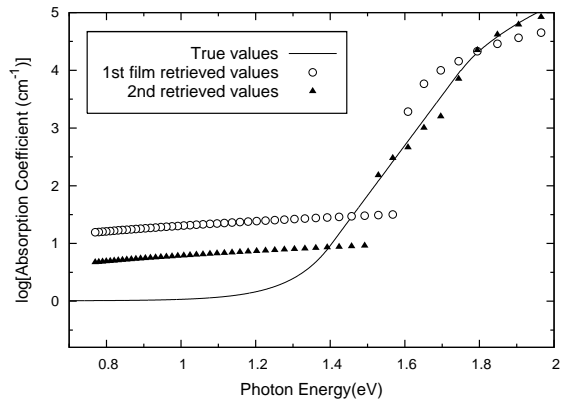
In this case, no underdeterminations appear. Figures 1, 2, 3 and 4 show the retrievals for systems AgB , BgD , CgB and CgD , respectively. Table 1 summarizes the retrieved thicknesses and the corresponding quadratic errors.



(a)

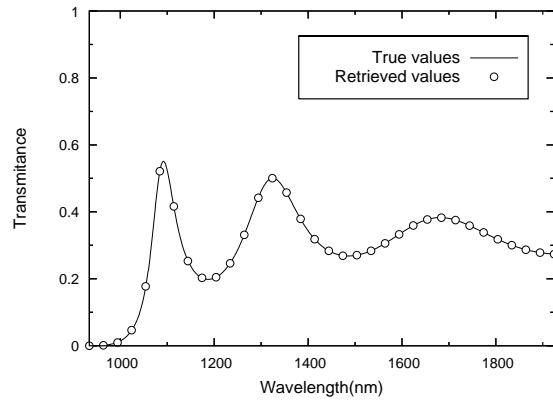


(b)

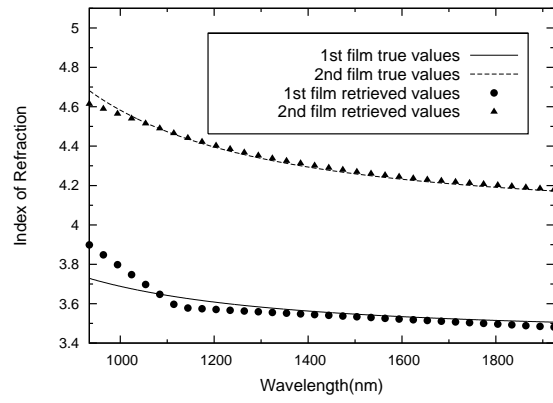


(c)

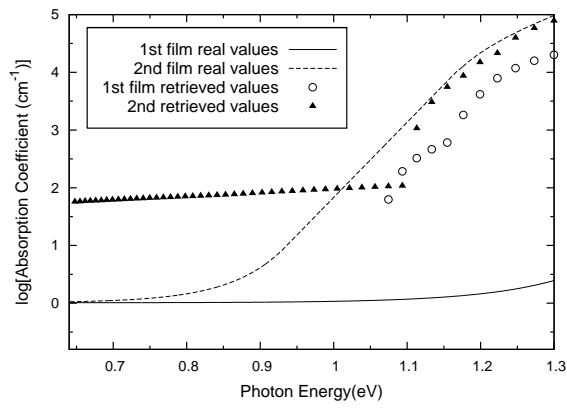
Figure 1: “True” and retrieved values of (a) the transmittance, (b) the refractive indices, and (c) the absorption coefficients of the numerically generated system AgB.



(a)

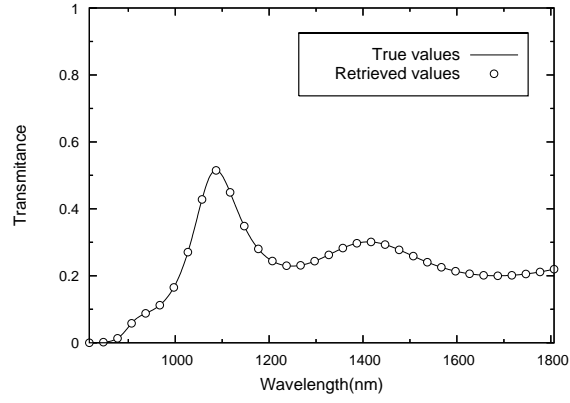


(b)

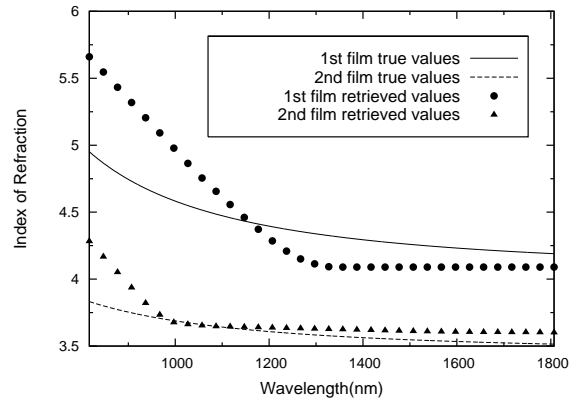


(c)

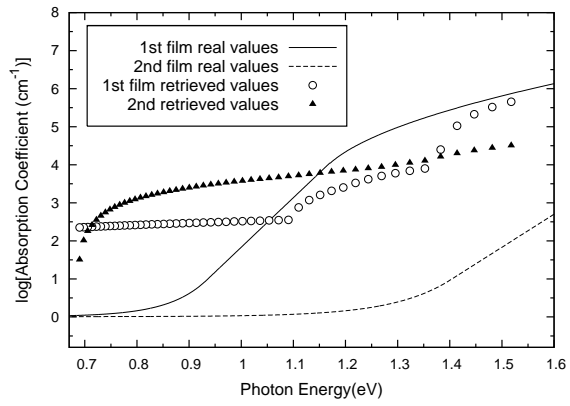
Figure 2: “True” and retrieved values of (a) the transmittance, (b) the refractive indices, and (c) the absorption coefficients of the numerically generated system BgD.



(a)

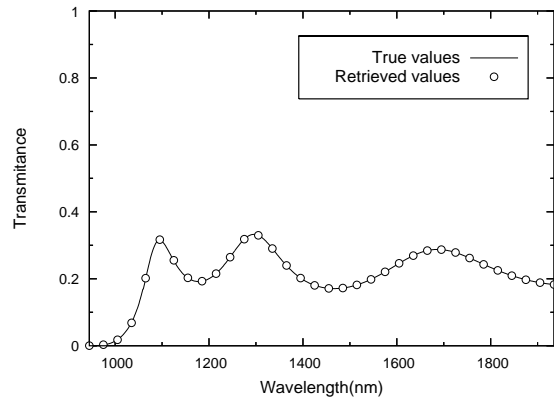


(b)

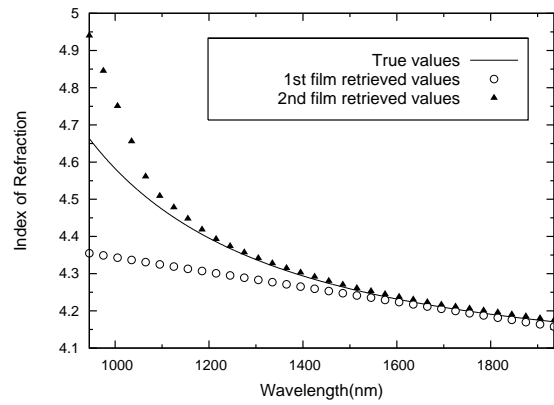


(c)

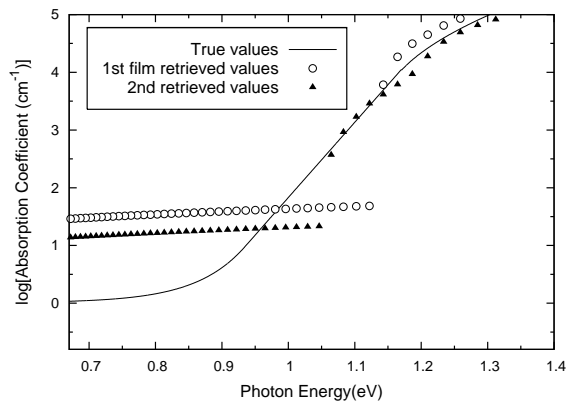
Figure 3: “True” and retrieved values of (a) the transmittance, (b) the refractive indices, and (c) the absorption coefficients of the numerically generated system CgB.



(a)



(b)



(c)

Figure 4: “True” and retrieved values of (a) the transmittance, (b) the refractive indices, and (c) the absorption coefficients of the numerically generated system CgD.

System	1st film		2nd film		Quadratic error
	d^{true}	d^{retr}	d^{true}	d^{retr}	
AgB	100	100	600	600	4.597773e-05
BgD	600	604	600	599	1.237465e-04
CgB	100	118	600	588	1.419527e-06
CgD	100	100	600	599	3.344105e-05

Table 1: Retrievals for systems AgB, BgD, CgB and CgD.

4.1.3 Experimental amorphous films

As a final test of the goodness and limitations of the algorithm, the retrieval program was applied to a real structure consisting of two films of different material. In what follows we describe the preparation of the two-films structure, the nature of the films and of the substrate, the transmittance of the single- and the double-film structures, and finally we discuss the quality of the retrieval.

The chosen structure consists of a both-sides polished high-quality crystalline silicon (c-Si) wafer supporting on one of its faces two amorphous semiconductor films of different nature. The first, on top of the c-Si substrate is a *ca.* $\sim 800\text{nm}$ thick hydrogen-free amorphous germanium (a-Ge) film. The second ($\sim 1150\text{nm}$ thick) going on top of the a-Ge layer is a H-free amorphous silicon (a-Si) film. Both films were deposited in an rf-sputtering system using semiconductor-quality targets and Ar as a ionizing gas. The deposition rate was of 0.1 nm/sec, the substrate being kept at 200 C during the whole process. The deposition times were 110 Min. and 180 Min. for the a-Ge and the a-Si films, respectively. During the deposition run, a-Ge and a-Si single layers were also deposited onto separate c-Si substrates. The transmittance of all films and of the substrate were measured with a Perkin Elmer Lambda 9 spectrophotometer in the 930-2750nm wavelength range. The goodness of the T data for wavelengths larger than 1500nm was confirmed independently with a Nicolet FTIR spectrophotometer. The idea behind the deposition of a-Ge and a-Si films identical to those composing the double structure was to compare the optical constants obtained with our well proven PUMA algorithm for single films [3], with those retrieved from the double-film structure.

The thickness of the three films was also estimated mechanically from a film-substrate step left by a clamp during deposition. The film-substrate step so obtained was not of perfect quality and Talystep measurements on different places gave slightly different values. We performed three measurements on the step and found the following average values: a-Si: single film $\sim 1150\text{nm}$; a-Ge single film $\sim 800\text{nm}$; double structure $\sim 1790\text{nm}$. As expected from the very different deposition times, the a-Si film is thicker than the a-Ge one. The difference between the sum of the thickness of the isolated semiconductor films and the thickness of the double structure may stem from experimental mechanical errors and from the sequence adopted to deposit the layers, which may alter their structure. We come back to the point when discussing the results of the retrieval process. Before considering the retrieval of the optical properties let us compare the mechanically measured thicknesses

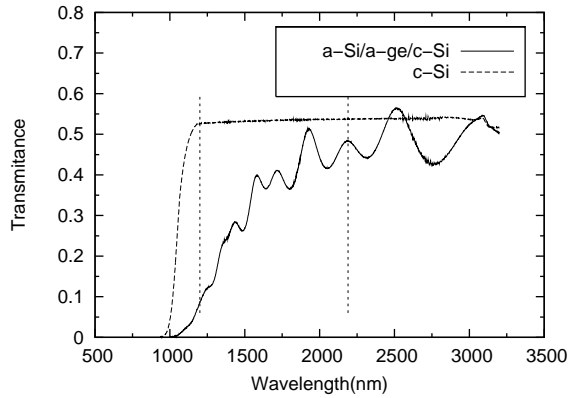
Film	Retrieved thicknesses (in nanometers)		
	Mechanical	Using PUMA for the single-film a-Si/c-Si and a-Ge/c-Si structures	Using PUMA for the double-film structure a-Si/a-Ge/c-Si
a-Si	1150	1135	1136
a-Ge	800	712	724
Both films	1790	–	1860

Table 2: Retrieved thicknesses of the single-film a-Si/c-Si and a-Ge/c-Si and the double-film a-Si/a-Ge/c-Si structures using PUMA and an independent mechanical method.

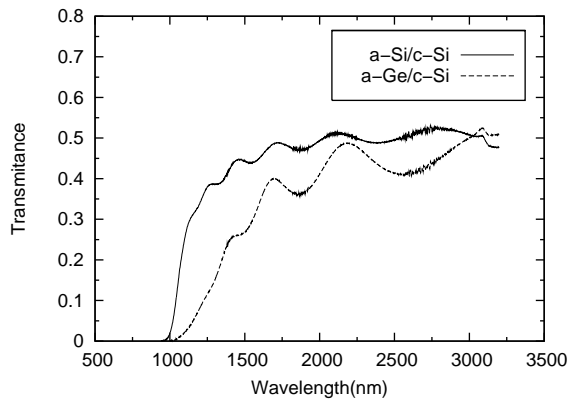
with those found from the retrieval algorithm. Table 2 shows the details. Let us note that the thicknesses retrieved from the single- and double-film structures agree remarkably well within experimental errors, as well as with the figures found by an independent mechanical method.

Figure 5(a) shows the transmittance of the c-Si substrate and of the double-film structure. Figure 5(b) displays the transmittance of the individual a-Si/c-Si and a-Ge/c-Si films, co-deposited with the double-film structure. As the retrieval algorithm assumes that the substrate is transparent, we have only performed calculations in the wavelength range comprised between the vertical dotted lines in Figure 5(a). So, the calculation to retrieve the films properties consider only the 1200–2190nm range. In this energy interval the refractive index of the c-Si substrate has been estimated from its transmittance [10]. As apparent from Figure 5(a-b), in the selected wavelength range the transmittance of the films possesses a well defined interference structure. As expected from the electronic structure and the refractive index difference between film and substrate, the single a-Si film has a higher transmittance in the whole wavelength range and the corresponding interference pattern is flatter than that of the a-Ge film [20]. As a consequence of this, the transmittance of the double-film structure is, to a certain extent, determined by the denser and less transparent germanium film.

Figure 6(a-b) and Table 2 compare, respectively, the retrieved optical constants and the thickness of the isolated a-Si and a-Ge semiconductor films with those obtained from the double-film structure. They indicate that: (i) There is a retrieval of two films having different optical constants. (ii) The retrieval of the thicknesses is remarkably good. (iii) Figure 6 also indicates that the retrieval of the optical constants is better for a-Ge than for a-Si; i.e., the film determining, or governing, the overall transmittance. (iv) In the case of a-Ge there is a perfect agreement between the retrieved refractive indices of both films (Figure 6(a)). On the contrary, the retrieved index of refraction of the a-Si film (Figure 6(a)) differs between the two structures by an almost constant factor of 0.3. Regarding the absorption coefficient we find that the amorphous germanium film is clearly recognized by the inversion algorithm, the retrieved α 's being identical between the two films within a factor of 2. The absorption coefficient of the a-Si film is also relatively well retrieved, except in the low energy photon region where the difference between structures



(a)



(b)

Figure 5: Transmittances of (a) the c-Si substrate and the double-film structure, and of (b) the single-film structures.

increases.

5 Discussion

5.1 Discussion on computer-generated films

We observed that the worst performance of our method occurs when the data are generated using two films of the same nature having the same thicknesses. The reason is given in Figure 7(a-i). Roughly speaking, what is apparent from Figure 7 is that in the symmetric structures the position of the transmittance extrema is less sensitive, or not sensitive at all, to thickness variations (see Figures 7(a-c)), whereas in the asymmetric structures, either because of film thickness difference or material composition (see Figures 7(d-i)), they produce important changes in the overall shape of the transmittance. Also, the variation of the transmittance with respect to small changes of the film thickness ($\pm\Delta d$)

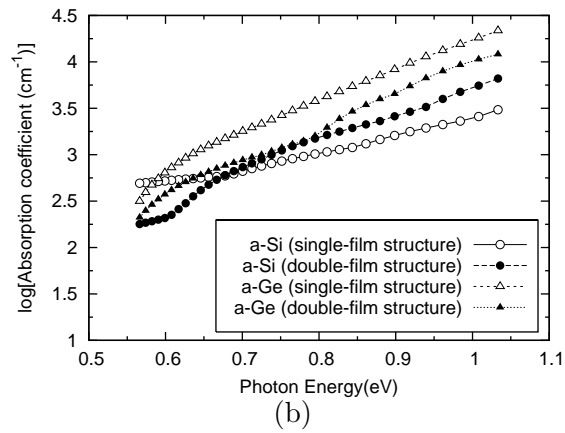
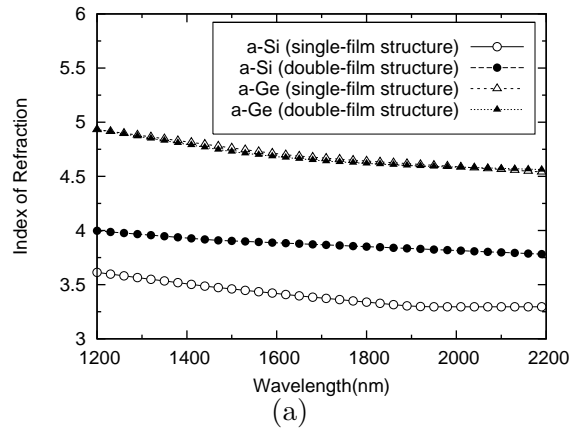


Figure 6: Retrieved optical constants of the a-Si and a-Ge semiconductor films using PUMA from the single-film and the double-film structure.

is smaller in the symmetric case. That means that the quadratic error, or target function of (3), is flatter when symmetry occurs in the FSF structure. The flatness of $QE(\pm\Delta d)$ is, of course, one of the main reasons for the bad retrieval of the true thicknesses.

On the other hand, the numerical experiments indicate the possibility of retrieving, from transmittance data, the optical constants and the thickness, despite the high under-determination of the problem. A few comments are in order.

- a) The thickness of the films is always retrieved within a surprising accuracy.
- b) Consider Figures 1 and 5; i.e., structures with two films of the same nature but different thickness, AgB and CgD, respectively. In both *gedanken* experiments the absorption coefficient of the material is correctly retrieved for values of α big enough to produce a detectable change in the transmittance. The retrieval of the index n is also very good, except in regions where the absorption dominates completely the transmittance.
- c) Consider Figure 2, corresponding to films of different nature but same thickness. In this case, the transmittance is dominated, so to speak, by the smallest gap material. So, the retrieved absorption corresponds to the more opaque film, the other film being more or less “transparent” in the overall transmittance interval. On the contrary, the index n is correctly retrieved for both materials in the considered wavelength range. See Figure 2.
- d) Figure 3 shows the numerical results of films of different nature and different thickness. In this particular case we have considered the structure a-Ge:H (100nm)/glass/a-Si:H (600nm). The absorption of the materials is different but the small gap material is much thinner than the large gap material. As a consequence, the contribution to the absorption of both films becomes of a similar magnitude and the algorithm cannot find neither of them. In spite of this fact, the refractive indices are more or less retrieved.

5.2 Discussion on experimental results

During the last decades, research work on the properties of amorphous semiconductors has clearly shown that the structural, optical and electrical properties of such materials strongly depend on deposition methods and conditions, including the chemical preparation and nature of the substrate [20, 21, 22]. Needless to say, such considerations apply to the properties of the a-Si and a-Ge films being discussed here. In this sense, we remark that when we state that the films of the single and the double structure are deposited under identical nominal conditions we just mean that they were deposited simultaneously, which does not mean that their structure is necessarily identical.

Let us make the point clear by considering each material separately. Hydrogen free amorphous germanium was deposited onto a couple of crystalline silicon wafers which, after growth, are nominally identical. However, one of them was taken out of the deposition chamber for optical measurements whereas the other remained in the chamber to be

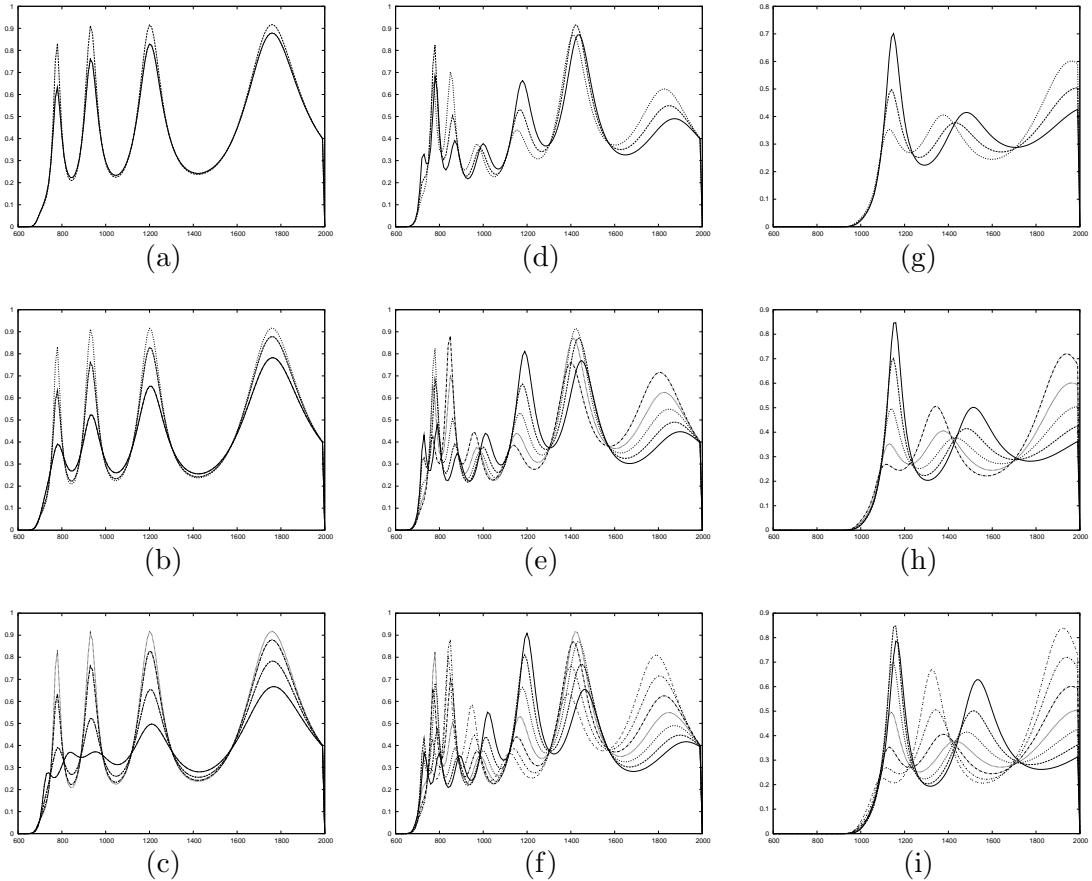


Figure 7: All figures correspond to systems with two films deposited onto different sides of a glass substrate and with $d_1 + d_2 = 1000\text{nm}$. The first “column” (pictures (a-c)) corresponds to films of the same material (a-Si:H) and the same thickness ($\bar{d}_1 = \bar{d}_2 = 500\text{nm}$). The second column corresponds to films of the same material (a-Si:H) and different thicknesses ($\bar{d}_1 = 200\text{nm}$ and $\bar{d}_2 = 800\text{nm}$). The third column corresponds to films of different materials (a-Si:H and a-Ge:H) and the same thickness ($\bar{d}_1 = \bar{d}_2 = 500\text{nm}$). Pictures in the first “line” correspond to transmittances generated varying $d_1 \in \{\bar{d}_1 - 10\text{nm}, \bar{d}_1, \bar{d}_1 + 10\text{nm}\}$ (remember that $d_1 + d_2 = 1000\text{nm}$). The two following lines correspond to variations of d_1 within an increasing range. It can be observed that in the case “same-material films with similar thicknesses” the variation in the transmittance is smaller than in the other cases. A possible explanation for this observation is the symmetry of the system that does not occur in the other situations.

covered by an amorphous silicon film. The deposition of the amorphous silicon layer was made onto a crystalline silicon wafer and on the substrate containing the a-Ge layer on top of it. It has to be noted here that the growth of this second film (a-Si) took three hours, during which the previously deposited a-Ge film annealed at 200 C. The annealing process contributes to modify its previous structural properties. The fact that thermal annealing changes the properties of amorphous semiconductors has been abundantly reported in the literature [23, 24]. Before the report on the beneficial effects of hydrogenation in removing deep defect states in the pseudo-gap of column IV amorphous semiconductors, thermal annealing was one of the methods used to improve the structure of amorphous germanium and silicon, in particular the size and density of internal voids. In other words, we do not expect the structural properties of the a-Ge films of the single- and of the double-film structure to be identical. Similar, although different considerations apply to the case of the simultaneous deposition of the a-Si film. One of the layers is deposited onto the ordered surface of a crystalline silicon wafer whereas the other grew onto the disordered surface of the previously deposited amorphous germanium film. It is also known that the structure and chemical nature of the substrate affects the properties of amorphous semiconductors [25]. The problem is that we do not know either the magnitude or the way these differences affect the optical properties of the present films.

Besides these considerations on the different optical response of the films stemming from their structure, we have also to consider experimental errors, absent in *gedanken* films. The errors originate from the fact that the H-free amorphous films are not perfectly flat, the presence of unavoidable voids provokes a rather rough surface [25]. Moreover, there are also errors from the measured transmittance which may be either random or systematic. They normally poison the transmittance data, as well as the noisy regions in the measured spectra. Finally, the retrieval algorithm possesses its own limitations which have been discussed in a previous section referring to computer-generated films.

6 Conclusions

The main conclusions of the present research concerning the retrieval of the optical constants of two superimposed films are the following:

- Compact formulae for the theoretical transmittance of a couple of different films deposited onto a transparent substrate were presented.
- The retrieval of the properties becomes very hard, if not impossible, when the structure contains films of identical nature and of the same thickness. An additional information concerning the thickness of one of the films is necessary for a good retrieval.
- For films made of the same material but having a different thickness the algorithm retrieves properly the properties and the thickness of the structure.
- The retrieval is also good when the films are of different material. In this case, as shown in the level-set graphics, the indetermination is drastically reduced. The

reason is that the Physical Constraints introduced in the model, although clearly insufficient for regularizing the same-film case, reduce the space of search in an efficient way in the case of two different films. In other words, the constraints play, in the two-different film structure, the same role played in the single-film situation.

- In general, the retrieval of the properties of different films indicates that the absorption coefficient is better retrieved for the denser film, the one that governs the transmittance. The index of refraction is normally well retrieved for both layers, particularly in the low absorption spectral regions.

Let us conclude saying that it is surprising that an inverse problem with such a high degree of underdetermination can be correctly solved with a minimization algorithm. To our knowledge this is the first report on the retrieval of the optical constants and the thickness of multiple-film structures using transmittance data only.

Acknowledgments

The authors are indebted to F. C. Marques - IFGW/UNICAMP for the deposition of amorphous films. This work has been partially supported by PRONEX - CNPq / FAPERJ E-26 / 171.164/2003 - APQ1 and by the Brazilian agencies FAPESP (Grants 06/53768-0 and 06/51827-9) and CNPq (PROSUL 490333/2004-4).

Appendix

Analytical expressions used to compute the substrates and the simulated optical constants of semiconductor and dielectric films:

$$s_{glass}(\lambda) = \sqrt{1 + (0.7568 - 7930/\lambda^2)^{-1}}.$$

$$s_{Si}(\lambda) = 3.71382 - 8.69123 \cdot 10^{-5} \lambda - 2.47125 \cdot 10^{-8} \lambda^2 + 1.04677 \cdot 10^{-11} \lambda^3.$$

a-Si:H

Index of refraction:

$$n^{\text{true}}(\lambda) = \sqrt{1 + (0.09195 - 12600/\lambda^2)^{-1}}.$$

Absorption coefficient:

$$\ln(\alpha^{\text{true}}(E)) = \begin{cases} 6.5944 \cdot 10^{-6} \exp(9.0846E) - 16.102, & 0.60 < E < 1.40; \\ 20E - 41.9, & 1.40 < E < 1.75; \\ \sqrt{59.56E - 102.1} - 8.391, & 1.75 < E < 2.20. \end{cases}$$

a-Ge:H

Index of refraction:

$$n^{\text{true}}(\lambda) = \sqrt{1 + (0.065 - (15000/\lambda^2))^{-1}}.$$

Absorption coefficient:

$$\ln(\alpha^{\text{true}}(E)) = \begin{cases} 6.5944 \cdot 10^{-6} \exp(13.629E) - 16.102, & 0.50 < E < 0.93; \\ 30E - 41.9, & 0.93 < E < 1.17; \\ \sqrt{89.34E - 102.1} - 8.391, & 1.17 < E < 1.50. \end{cases}$$

In the expressions above, the wavelength λ is in nm, the photon energy $E = 1240/\lambda$ is in eV, and the absorption coefficient α is in nm^{-1} .

References

- [1] I. Chamboleyron and J. M. Martínez, Optical properties of dielectric and semiconductor thin films, *Handbook of Thin Films Materials* edited by H. S. Nalwa, Ch. 12, Volume 3, Academic Press, pp. 593–622 (2001).
- [2] D. Poelman and P.F. Smet, Methods for the determination of the optical constants of thin films from single transmission measurements: a critical review, *Journal of Physics D: Applied Physics* 36, pp. 1850–1857 (2003).
- [3] E. G. Birgin, I. Chamboleyron and J. M. Martínez, Estimation of the optical constants and the thickness of thin films using unconstrained optimization, *Journal of Computational Physics* 151, pp. 862–880 (1999).
- [4] M. Mulato, I. Chamboleyron, E. G. Birgin and J. M. Martínez, Determination of thickness and optical constants of amorphous silicon films from transmittance data, *Applied Physics Letters* 77, pp. 2133–2135 (2000).
- [5] I. Chamboleyron, S. D. Ventura, E. G. Birgin and J. M. Martínez, Optimal constants and thickness determination of very thin amorphous semiconductor films, *Journal of Applied Physics* 92, pp. 3093–3102 (2002).
- [6] S. D. Ventura, E. G. Birgin, J. M. Martínez and I. Chamboleyron, Optimization techniques for the estimation of the thickness and the optical parameters of thin films using reflectance data, *Journal of Applied Physics* 97, 043512 (2005).
- [7] E. G. Birgin, I. Chamboleyron and J. M. Martínez, Optimization problems in the estimation or parameters of thin films and the elimination of the influence of the substrate, *Journal of Computational and Applied Mathematics* 152, pp. 35–50 (2003).
- [8] M. Born, E. Wolf, *Principles of Optics*, Pergamon Press (1st Ed. 1959).
- [9] O. S. Heavens, *Optical Properties of Thin Solid Films*, Butterworths Scientific Publications, London (1950).

- [10] R. Swanepoel, Determination of the thickness and optical constants of amorphous silicon, *Journal of Physics E: Scientific Instruments* 16, pp. 1214–1222 (1983).
- [11] T. C. Paulick, Inversion of normal-incidence (R,T) measurements to obtain $n+ik$ for thin films, *Applied Optics* 25, pp. 562–564 (1986).
- [12] H. M. Liddell, *Computer-aided techniques for the design of multilayer filters*, Adam Hilger, Bristol, UK (1980).
- [13] S. D. Ventura, Optimization techniques for film parameter estimation, *Ph.D. Thesis*, Department of Applied Mathematics, University of Campinas (2004).
- [14] M. Raydan, The Barzilai and Borwein gradient method for the large unconstrained minimization problem, *SIAM Journal on Optimization* 7, pp. 26–33 (1997).
- [15] E. G. Birgin and J. M. Martínez, A spectral conjugate gradient method for unconstrained optimization, *Applied Mathematics and Optimization* 43, pp. 117–128 (2001).
- [16] B. Akaoglu, I. Atilgan and B. Katircioglu, Thickness and optical constant distributions of PECVD a-SiCx : H thin films along electrode radial direction, *Thin Solid Films* 437, pp. 257–265 (2003).
- [17] E. G. Birgin, I. Chambouleyron, J. M. Martínez and S. D. Ventura, Estimation of optical parameters of very thin films, *Applied Numerical Mathematics* 47, pp. 109–119 (2003).
- [18] F. Curiel, W. E. Vargas and R. G. Barrera, Visible spectral dependence of the scattering and absorption coefficients of pigmented coatings from inversion of diffuse reflectance spectra, *Applied Optics* 41, pp. 5969–5978 (2002).
- [19] A. Ramirez-Porras and W. E. Vargas-Castro, Transmission of visible light through oxidized copper films: feasibility of using a spectral projected gradient method, *Applied Optics* 43, pp. 1508–1514 (2004).
- [20] N. F. Mott and E. A. Davis, *Electronic properties in non crystalline materials*, Clarendon Press, Oxford (1979).
- [21] G. Dalba, P. Fornasini, R. Grisenti, F. Rocca, I. Chambouleyron and C. F. O. Graeff, Local order in hydrogenated amorphous germanium thin films studied by EXAFS, *Journal of Physics: Condensed Matter* 9, pp. 5875–5888 (1997).
- [22] A. R. Zanatta M. Mulato and I. Chambouleyron, Exponential absorption edge and disorder in Column IV amorphous semiconductors, *Journal of Applied Physics* 84, pp. 5184–5190 (1998)
- [23] M. H. Brodsky, D. M. Kaplan and J. F. Ziegler, *Proc. 11th Int. Conf. on the Physics of Semiconductors*, Warsaw, p. 529, PWN-Polish Scientific Publishers, Warsaw (1972).

- [24] W. Paul, G. A. N. Connell and R. J. Temkin, Amorphous germanium; A model for the structural and optical properties, *Advances in Physics* 22, pp. 529–580 (1973).
- [25] T. M. Donovan and K. Heinemann, High-resolution electron microscope observations of voids in amorphous Ge, *Physical Review Letters* 27, 1794–1796 (1971).